MODELING OF THE SPATIAL FACIES DISTRIBUTION BY MARKOV RANDOM FIELDS

HÅKON TJELMELAND
Department of Mathematical Sciences,
Norwegian University of Science and Technology,
Trondheim, Norway

Abstract. Markov random fields (MRFs) have been suggested as a model for the spatial distribution of sedimentary facies in petroleum reservoirs. However, unfavorable large-scale properties of common MRFs have restrained their popularity for reservoir characterization. In this article, we review a class of MRFs with more realistic large-scale properties and present simulation examples.

1. Introduction

The spatial distribution of sedimentary facies in petroleum reservoirs has a major influence on the fluid flow, and thereby on the production of oil and gas. Two classes of phenomena can be defined, event and mosaic phenomena; see Haldorsen and Damsleth (1990), Omre (1991), Ripley (1992) and Dubrule (1993). The first class represents occurrences of facies objects in a background matrix. Typical examples are shale units in a sand matrix (Haldorsen and Lake, 1984; Syversveen and Omre, 1994) and river-beds in a non-permeable background (Georgsen and Omre, 1993). Mosaic phenomena represent packing of different facies, but no natural background facies exist. With a natural ordering of the facies, a truncated continuous random function form a reasonable model; see Matheron et al. (1987). However, if no reasonable ordering of the facies exist, Markov random fields (MRFs) appear as the natural choice of models to consider.

MRFs have been extensively used as prior distributions in Bayesian image analysis (Geman and Geman, 1984; Besag, 1986). The attention has mainly been restricted to pairwise interaction models, with the Ising and Potts models as typical examples. It is well known that realizations from these models exhibit, for many application, totally unrealistic large-scale properties. They are still frequently used in image analysis, because of favorable local properties. Moreover, observations cover the entire area of interest and this correct for the unfavorable large-scale properties. However, in reservoir characterization observations are sparse and this makes it essential to use a model which reflects the properties of the phenomenon under study. One should note that some scenes shown in the literature are not representative for the pairwise interaction MRFs they claim to represent. Instead, they are results from Markov chain runs that have not converged.

A large number of higher-order interaction MRFs is possible and several classes have been suggested to obtain models with realistic large-scale properties. Tjelmeland and Holden (1993) define semi-MRFs, where the probability distribution is a function of the size and form of the objects; see also Møller and Waagepetersen (1996). This seems a natural approach, but the resulting models suffer from slow convergence of the Markov chain simulations. Johnson (1994) also considers MRFs with higher-order interactions, but seems unable to control large-scale structures in the realizations. In this paper, we adopt the approach of Tjelmeland and Besag (1996), where higher-order interactions are introduced in a methodical fashion, and define models suitable for the spatial distribution of sedimentary facies in petroleum reservoirs.

2. Markov random fields

For a general introduction to MRFs, see Besag (1974) or Cressie (1993). Here, we give a brief introduction to the basic notions of MRFs.

2.1. DEFINITION AND NOTATION

Consider a regular lattice of n nodes and number the nodes from one to n. Let i denote a typical node, with $i \in SS = \{1, \ldots, n\}$. To each node, i, there is associated a value, x_i, representing facies value. Let K denote the number of facies and set $x_i \in \Lambda = \{0, 1, \ldots, K-1\}$. A facies configuration on the entire lattice is given by $x = (x_1, \ldots, x_n) \in \Omega = \Lambda^n$. To denote facies values in a set $A \subset SS$, we use x_A.

To each node $i \in SS$ there is associated a set of neighboring nodes, denoted by ∂i. The neighborhood is required to be symmetric, i.e. $i \in \partial_j \Leftrightarrow j \in \partial_i$. Nodes i and j are said to be neighbors if $i \in \partial j$. A stochastic field, X, with distribution $\pi(x) = \text{Prob}\{X = x\}, x \in \Omega$ is a MRF if

$$\pi(x_i | x_j; j \neq i) = \pi(x_i | x_{\partial i}). \tag{1}$$

The neighborhoods, $\partial 1, \ldots, \partial n$, give the cliques of the system. A clique is a maximal set of nodes, in which each distinct pair of nodes are neighbors. With the addition of the minor positivity condition, $\pi(x) > 0$ for all $x \in \Omega$, it follows from the Hammersley-Clifford theorem (Besag, 1974) that the joint distribution for X must take the form

$$\pi(x) = c \cdot \exp\left\{-\sum_C V_C(x_C)\right\}, \tag{2}$$

where the sum is over all cliques C, and $V_C(\cdot)$ are arbitrary finite functions, often called potential functions.

In this article we restrict the attention to potential functions of the form

$$V_C(x_C) = \begin{cases} \theta_l & \text{if } x_C \in \mathcal{D}_l \text{ for } l = 1, \ldots, L \\ 0 & \text{otherwise,} \end{cases} \tag{3}$$

where $\theta = (\theta_1, \ldots, \theta_L)$ is a parameter vector of dimension L and $\mathcal{D}_1$, ..., $\mathcal{D}_L$ are sets of configurations in a clique. Examples of L, θ and $\mathcal{D}_1, \ldots, \mathcal{D}_L$ are given in the next section. With the potential function given in equation (3), the joint distribution gets the simpler form

$$\pi(x) = c \cdot \exp\left\{-\sum_{l=1}^{L} \theta_l \cdot n_l(x)\right\}, \tag{4}$$

where $n_l(x)$ is the number of cliques with configurations in the set $\mathcal{D}_l$.

2.2. SIMULATION ALGORITHM

Unfortunately, there exist no direct methods for simulation of MRFs. Instead, iterative simulation algorithms must be used; see Besag et al (1995) and references therein. The realizations presented in this article are generated by a simple Metropolis algorithm (Metropolis et al., 1953). Each iteration consists of two steps. First, a potential new facies configuration is constructed by replacing the current facies value in a randomly selected node with a new one, uniformly sampled from the $K-1$ available values. Second, the new configuration is accepted with probability

$$\alpha(x \to x^\star) = \min\left\{1, \frac{\pi(x^\star)}{\pi(x)}\right\}, \tag{5}$$

where x and $x^\star$ are the current and the potential new configurations, respectively. This procedure defines a Markov chain and can be shown to converge to the MRF specified; see the references mentioned.

2.3. CONDITIONING

The ability to generate realizations conditioned on observations is crucial in reservoir characterization. Observations can either be exact, as core samples from wells, or associated with uncertainty, as logs and seismic data.

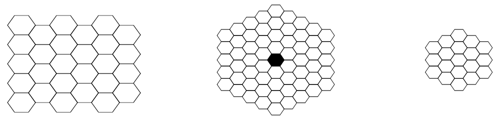

(a) (b) (c)

Figure 1. (a) A part of a hexagonal array. Each node are surrounded by six nodes, (b) the fourth order neighborhood used in the shale barrier model, and (c) corresponding form for the interior cliques.

Both kind of observations can easily be taken into account in simulation of MRFs. In the simulation procedure specified above, exact observations are reproduced by fixing the facies values for nodes with observations. To include observations associated with measurement error, the relation between the unknown truth and the data must be modeled by a likelihood function. This is the standard Bayesian approach, see the discussion in Omre and Tjelmeland (1996).

3. A model for extensive shales barriers

Flow barriers of large lateral extent are present in some petroleum reservoirs. They are typically observed in a large number of wells and it is often possible to correlate the observations over large parts of the field; see Omre et al. (1993) and MacDonald and Halland (1993).

The vertical position of the barriers are often well understood from well observations and general geological knowledge. Here, we assume it to be known or modeled separately, so that the modeling becomes a 2D problem. Furthermore, we restrict the attention to thin barriers. Thus, the thickness can be ignored and the barrier can be represented by a binary field $X = (X_1, \ldots, X_n)$, where $X_i = 0$ and 1 represents presence and absence of barrier in node i, respectively.

3.1. MODEL SPECIFICATION

In the model for shale barriers, we use a hexagonal array. A similar model for a rectangular lattice can easily be devised, but nicer symmetry relations are present in the hexagonal array; see Figure 1(a). For the interior nodes, a fourth order neighborhood is used where each node has sixty neighbors, see Figure 1(b). Nodes close to the edge of the array have fewer neighbors, and this is discussed separately below. This gives interior cliques that consist of nineteen pixels; see Figure 1(c). From the examples below, it should become clear that cliques of this size are sufficiently large to enable modeling of realistic structures. But it is also small enough to allow efficient simulation.

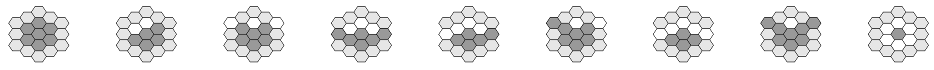

(a) (b) (c) (d) (e) (f) (g) (h) (i)

Figure 2. Configurations defining the potential function for shale barrier model; see Table 1. Black and white represent barrier and non-barrier, respectively. Values in gray nodes are ignored.

l	$\mathcal{D}_l$	$V_C(x_C)$	type of configuration
1	(a)	θ_1	interior shale
2	(b) (c) (d)	θ_2	straight shale edge
3	(e)	θ_3	30^o convex corner
4	(f)	θ_4	30^o concave corner
5	(g)	θ_5	60^o convex corner
6	(h)	θ_6	60^o concave corner
7	(i)	θ_7	single shale node
8	other conf. with shale in central node	θ_8	other

TABLE 1. The parameterization of the potential function for a 19-clique. Configurations (a) to (i) refers to the configurations shown in figure 2. Rotations and reflections of the specified configurations are also included in the sets.

To specify the configuration sets $\mathcal{D}_1, \ldots, \mathcal{D}_L$, which define the potential functions, we focus on shale areas and include in the sets only configurations with shale in the central node. Thus, the potential is zero whenever a clique has non-shale in the central node. Moreover, we use $L = 8$ and let the various sets correspond to eight different roles of the center node, see the specification in Table 1 and Figure 2.

To specify reasonable potential functions for cliques on the edge of the array is often problematic in MRFs. Obviously, one would prefer that the statistical properties of the field is the same close to the boundary of the array as in the interior. One possibility is to use periodic boundary conditions, i.e. to let nodes on the boundary be neighbors of nodes on the opposite boundary. This is a reasonable choice in a model exploration phase, but introduce unrealistic correlations when used for real phenomena. Another approach is to simulate on a larger lattice and discard the extra nodes. This eliminate the edge effects in the area of interest if sufficiently extra nodes are added, but require more computer resources for simulation. Here, we chose a third approach. Also for each node close to the edge of the array, we consider one 19-clique centered at the node. Some of the nineteen nodes is then outside the array and their values therefore are undefined. We let

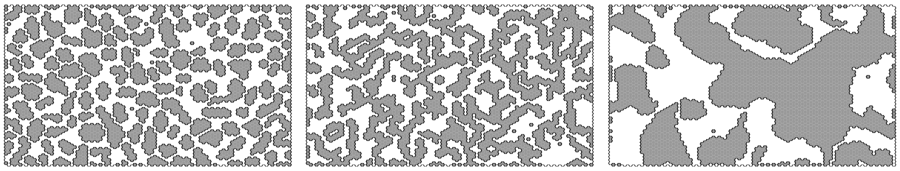

(i) (ii) (iii)

Figure 3. Map view of realizations from the shale barrier model on a grid with 5,000 nodes and for three different parameter sets.

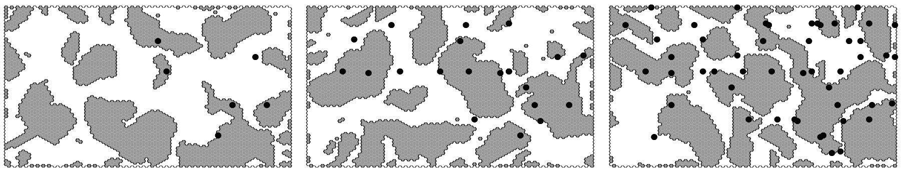

Figure 4. Map view of conditional realizations from the shale barrier model on a grid with 5,000 nodes. The realizations are conditioned on 6, 20 and 50 observations, respectively, where observations are marked with blobs.

the potential functions of such cliques be given from the potential function specified in Table 1 by taking the maximum over all possible combinations of facies values in nodes with undefined values.

3.2. SIMULATION EXAMPLES

In this section we provide realizations from the specified model for various parameter values. Figure 3 contains three realizations based on the parameter vectors (i) $\theta = (0.144, 0.330, -0.704, 1.346, 0.464, 1.941, 3.338, 4.492)$, (ii) $\theta = (0.288, 0.593, 0.263, 0.390, 0.715, 0.613, 3.621, 4.872)$ and (iii) $\theta = (-0.0107, 0.520, 0.763, 1.286, 2.763, 2.524, 4.030, 5.751)$, respectively; see section 5 for the procedure used to chose the parameter values. The three realizations presented demonstrate that the parameterization chosen allow a large variation in the geometric structure of the shale areas. One should note that the realizations are not conditioned on the coverage ratio of shale, which varies stochastically in the realizations. However, the parameter values specified above are chosen to give expected value equal to a half.

Figure 4 contains three realizations from the model with parameter vector (iii) specified above and conditioned on 6, 20 and 50 well observations, respectively. The values used for conditioning are selected independently at random. One can observe that the model is sufficiently flexible to allow the data to be reproduced without creation of artifacts in the realizations.

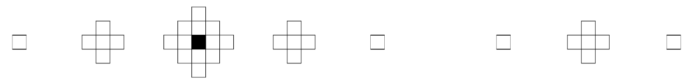

Figure 5. (a1)–(a5) The 24 neighbors for an interior node on five different node layers, and (b1)-(b3) a clique of seven nodes on three node layers.

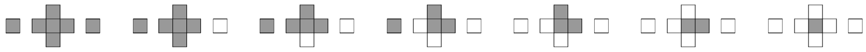

Figure 6. Configurations used in the definition of the potential function in the mosaic model; see also Table 2.

4. Three-dimensional mosaic model

In this section we demonstrate how the approach used in the previous section can be generalized to a three dimensional lattice.

4.1. MODEL SPECIFICATION — TWO FACIES

There exist no 3D lattice with the nice symmetry relations found in the 2D hexagonal array. We therefore use a rectangular lattice for our 3D models. In this grid, let two nodes be neighbors if the distance between them is less than or equal to two times the node distance. This gives that each interior node has 24 neighbors and cliques of size seven; see figure 5.

In the first model, assume that there are only two facies and denote them by A and B, respectively. Moreover, let the field be isotropic relative to the lattice. However, anisotropy is included if different grid resolution is used in the three coordinate directions. Finally, consider $L = 14$ different classes of clique configurations. The first seven classes have facies A in the center node and, similarly, the seven last classes have facies B in the center node; see figure 6 and Table 2. One should note that, as for the 2D MRF in section 3, the configuration classes are chosen to represent typical clique configurations in the type of realizations one want to generate. Potential functions for cliques at the boundary of the lattice are induced by the potentials for the interior cliques, as for the 2D shale barrier model.

4.2. SIMULATION EXAMPLE

This section contains a simulation example from the two-facies model specified above. The size of the lattice is $40 \times 40 \times 40$ and Figure 7 displays four vertical cross-sections through a realization from the model with param-

$\mathcal{D}_l$	$V_C(x_C)$	type of configuration
(a)	θ_1^c	interior
(b)	θ_2^c	straight edge
(c)	θ_3^c	2D corner
(d)	θ_4^c	3D corner
(e)	θ_5^c	sharp corner
(f)	θ_6^c	dead end
(g)	θ_7^c	single node

TABLE 2. The parameterization of the potential function for a 7-clique. c is facies A or B and configurations (a) to (g) refers to the configurations shown in figure 2. For c =A, dark and white in the figure represent facies A and B, respectively. For c =B, it is reversed, dark represent facies B and white A. Rotations of the specified configurations are also included in the sets.

Figure 7. Parallel vertical cross-sections through a realization from the mosaic model with three facies. The cross-sections are separated by two grid nodes in the order, upper left, upper right, lower left and lower right.

eters $(\theta_1^c, \ldots, \theta_7^c) = (-2.0, -2.0, -1.6, -1.2, 1.0, 1.5, 5.0)$ for c equal to A and B. To obtain anisotropy in the model, different grid resolution is used in horizontal and vertical directions. One should note that with $\theta_l^A = \theta_l^B$ for $l = 1, \ldots, 7$ as used here, the two facies are exchangeable.

4.3. MODEL SPECIFICATION — MORE THAN TWO FACIES

In this section we generalize the mosaic model of the previous section to allow specification of border relations and to include more than two facies. Let the lattice and neighborhood structure be unchanged. To simplify notation and to limit the number of parameters it is convenient to specify the potential function in a slightly different manner than before. Thus, let the potential for any clique configuration be given as a sum of three terms, $V_C(x_C) = \theta(x_C) + \beta_u(x_C^0, x_C^u) + \beta_l(x_C^0, x_C^l)$, where x_C^0, x_C^u and x_C^l denote the facies of the central node and the nodes above and below the central node of the clique, respectively. The two last terms, $\beta_u(\cdot,\cdot)$ and $\beta_l(\cdot,\cdot)$, specify

Figure 8. Parallel vertical cross-sections through a realization from the mosaic model with two facies. The cross-sections are separated by two grid nodes in the order, upper left, upper right, lower left and lower right.

preference for specific border relations, whereas the first term, $\theta(\cdot)$, is defined similarly as the potential function of the previous section. However, each the configuration classes corresponding to parameters θ_3^c and θ_4^c are divided in two subsets, one for configurations with only two facies present in x_C and for the remainder. Denote the corresponding potentials by $\theta_{3,ii}^c$, $\theta_{3,>ii}^c$, $\theta_{4,ii}^c$ and $\theta_{4,>ii}^c$, respectively. Again, the potential functions for cliques at the boundary of the lattice are induced from the interior potentials.

4.4. SIMULATION EXAMPLE

This section contains a simulation example from the specified model with three facies, denoted by A, B and C, respectively. Facies A and B should have approximately the same properties as in the previous example, whereas facies C is thinner and have a strong tendency to lie above A and below B.

Figure 8 displays four vertical cross-sections through a realization from the model. Equal parameters are used for facies A and B, namely $(\theta_1^c,\ \theta_2^c,\ \theta_{3,ii}^c,\ \theta_{3,>ii}^c,\ \theta_{4,ii}^c,\ \theta_{4,>ii}^c,\ \theta_5^c,\ \theta_6^c,\ \theta_7^c) = (-2.0, -1.98,\ -1.6,\ -1.8,\ -1.2, -1.6, 1.0, 1.5, 5.0)$ for c equal to A and B. For facies C, slightly different values are used, $(\theta_1^C,\ \theta_2^C,\ \theta_{3,ii}^C,\ \theta_{3,>ii}^C,\ \theta_{4,ii}^C,\ \theta_{4,>ii}^C,\ \theta_5^C,\ \theta_6^C,\ \theta_7^C) = (-1.9,\ -1.98,\ -1.8,\ -1.8, -1.6, -1.6, 1.0, 1.5, 5.0)$. The above specified border relations was included in the model by the parameter choice $\beta_u(C,A) = \beta_l(C,B) = 1.0$ and $\beta_u(C,B) = \beta_l(C,A) = -0.1$. Finally, to obtain thinner objects of facies C, $\beta_u(C,C) = \beta_l(C,C) = 1.0$ are used. The $\beta_u(\cdot,\cdot)$ and $\beta_l(\cdot,\cdot)$ for other values of the arguments are all zero.

5. Parameter estimation

Model parameters in MRFs have no clear geometric interpretation. Clearly, a lower value for θ_l gives higher probability for clique configurations in $\mathcal{D}_l$, but the parameter has no explanation as expectations or variogram functions in Gaussian random fields. This makes it especially important to have some automatic procedure for specification of models with specified properties or, alternatively, to estimate the parameters from available data.

5.1. MAXIMUM LIKELIHOOD ESTIMATION

First consider parameter estimation from an observed facies configuration, denoted by $y = (y_1, \ldots, y_n)$. A standard procedure for parameter estimation in statistics is to utilize the maximum likelihood principle; see, for example, Mardia et al. (1979) and Cressie (1993). The likelihood function, $l(\theta)$, if defined as the probability for observing what has actually been observed as function of the model parameters, i.e. $l(\theta) = \pi(y|\theta)$. As an estimate for θ one chose the θ which maximize "the likelihood" of the observed data, i.e., $\theta^\star = \text{argmax}\{l(\theta)\}$, where $\theta^\star$ denotes the maximum likelihood estimator (MLE). However, for many spatial models, including the MRFs considered here, it is difficult to decide the MLE because the normalizing constant, which is a function of the parameter vector θ, cannot be computed; see the discussion in Omre and Tjelmeland (1996). As a computational simpler alternative, it has therefore been suggested to replace the likelihood function with a pseudo-likelihood function; see Besag (1975). However, experience shows that this does not produce reliable results for the type of MRFs and grid sizes considered here; see Tjelmeland (1996).

With recent increasing computer power, it has become possible to obtain good approximations to the MLE also in models where the normalizing constant cannot be computed. One possibility is to use stochastic approximation techniques; see Younes (1991). Alternatively, one can estimate the normalizing constant by stochastic simulation; see Geyer and Thompson (1992), Geyer (1994) and Geyer and Møller (1994). For an example where the latter approach is used for parameter estimation from outcrop data, see Tjelmeland and Besag (1996).

5.2. SPECIFICATION OF GENERAL GEOLOGIC KNOWLEDGE

If no data from analogue geology is available, the maximum likelihood approach can still be utilized to specify parameter values in accordance with general geologic knowledge. To see how this can be done, one should first note the following two properties for MLE from distributions with the exponential form given in equation (4). First, the likelihood, and thereby also the MLE, is only a function of y through the statistics $n(y) = (n_1(y), \ldots, n_L(y))$. Second, for the model with θ given by the MLE, one has $\mathrm{E}_{\theta^\star}\{n_l(X)\} = n_l(y)$ for $l = 1, \ldots, L$.

Thus, parameter values are uniquely specified by the expected number of clique-configurations in each of the sets $\mathcal{D}_1, \ldots, \mathcal{D}_L$. To our experience, it is much easier to specify these expected values to obtain a model with the required properties than to specify the model parameters directly. The parameters in the shale barrier example are obtained by this approach. On a lattice of $1,800$ nodes, the expected values, $\mathrm{E}\{n(X)\}$, are

(i) $(260, 223, 230, 30, 130, 5, 20, 2)$, (ii) $(208, 250, 130, 130, 80, 20, 2)$ and (iii) $(652, 138, 55, 35, 6, 6, 6, 2)$, respectively. One should note that the specified numbers sum up to 900 in all three cases. Thus, because all clique configurations in $\mathcal{D}_1, \ldots, \mathcal{D}_L$ have shale in the central node, the expected fraction of shale becomes equal to a half.

6. Closing remarks

The examples presented in this paper demonstrate how to specify 2D- and 3D-MRFs with realistic large-scale properties. However, more experimentation with the models and different parameterizations are necessary in order to find models suitable for specific depositional environments.

In this paper, the focus is on the model and examples of realizations. MRFs must be simulated by iterative simulation algorithms and a very important question for such algorithms, is to decide the number of iterations necessary for convergence. To stop prematurely can result in scenes that are not at all representative for the specified model. To check whether convergence has been reached for the simulations presented in this paper, we used output analysis (Ripley, 1983) from runs with different initial configurations; see also the discussion in Tjelmeland and Besag (1996).

With the simulation algorithm used, which change the value in only one node in each iteration, the shale barrier model, with $5,000$ nodes, requires approximately 40 cpu-minutes, on an standard work station, to converge. The 3D mosaic model, where the number of nodes is much higher, requires many cpu-hours. However, other Metropolis-Hastings algorithms, which change values in many pixels simultaneously, may speed up the convergence.

Acknowledgment

The work is financed by a Ph.D. grant from the Research Council of Norway.

References

Besag, J. (1974). "Spatial interaction and the statistical analysis of lattice systems (with discussion)", *J. Royal Statist. Soc. B,* **36**,192-236.

Besag, J. (1975). "Statistical analysis of non-lattice data", *The Statistician*, **24**, 179-195.

Besag, J. (1986). "On the statistical analysis of dirty pictures (with discussion)", *J. Royal Statist. Soc. B,* **48**,259-302.

Besag, J., Green, P., Higdon, D. and Mengersen, K. (1995). "Bayesian computation and stochastic systems (with discussion)", *Statistical Science*, **10**, 3-66.

Cressie, N.A.C. (1993). *Statistics for Spatial Data.* Wiley, New York, 900p.

Dubrule, O. (1993). "Introducing more geology in stochastic reservoir modelling", in Soares, A. (ed.) *Geostatistics Tróia '92*, Kluwer Academic Publishers, 351-369.

Geman, S. and Geman, D. (1984). "Stochastic relaxation, Gibbs distributions, and the Bayesian restoration of images", *IEEE Trans. PAMI*, **6**, 721-741.

Georgsen, F. and Omre, H. (1993). "Combining fibre processes and Gaussian random functions for modelling fluvial reservoirs", in Soares, A. (ed.) *Geostatistics Tróia '92*, Kluwer Academic Publishers, 425-439.

Geyer, C.J. (1994). "Estimating normalizing constants and reweighting mixtures in Markov chain Monte Carlo", Technical report No. 568, School of Statistics, University of Minnesota.

Geyer, C.J. and Møller, J. (1994). "Simulation procedures and likelihood inference for spatial point processes", *Scand. J. of Stat.*, **21**, 359-373.

Geyer, C.J. and Thompson, E.A. (1992). "Constrained Monte Carlo maximum likelihood for dependent data (with discussion)", *J. Royal Statist. Soc. B*, **54**, 657-699.

Haldorsen, H.H. and Damsleth, E. (1990). "Stochastic modeling". *J. of Petroleum Technology*, 404-412.

Haldorsen, H.H. and Lake, L.W. (1984). "A new approach to shale management in field-scale models", SPEJ, August 1984, 447-457.

Johnson, V.E. (1994). "A model for segmentation and analysis of noisy images", *J. Amer. Statist. Assoc.,* **89**, 230-241.

MacDonald, A.C. and Halland, E.K. (1993). "Sedimentology and shale modeling of a sandstone-rich fluvial reservoir: Upper Statfjord formation, Statfjord field, northern North Sea", *The American Association of Petroleum Geologists Bull.*, **77**, 1016-1040.

Mardia, K.V., Kent, J.T. and Bibby, J.M. (1979). *Multivariate Analysis*, Academic Press, London, 518p.

Matheron, G., Beucher, H, de Fouquet, Ch., Galli, A., Guérillot, D. and Ravenne, Ch. (1987). "Conditional simulation of the geometry of fluvial-deltaic reservoirs", paper SPE 16753, presented at the 1987 SPE Annual Technical Conference and Exhibition, Dallas, sept. 27.-30.

Metropolis, N., Rosenbluth, A.W., Rosenbluth, M.N., Teller, A.H. and Teller, E. (1953). "Equations of state calculations by fast computing machines", *J. Chem. Phys.* **21**, 1087-1092.

Møller, J. and Waagepetersen, R. (1996). "Markov connected component fields", Technical report, Department of Mathematics and Computer Science, R-96-2009, University of Aalborg, Denmark, 37p.

Omre, H. (1991). "Stochastic models for reservoir characterization", in Kleppe, J. and Skjæveland, S.M. (eds.) *Recent advances in improved oil recovery methods for North Sea sandstone reservoirs*, Norwegian Petroleum Directorate, Stavanger, Norway.

Omre, H. and Tjelmeland, H. (1996). "Petroleum Geostatistics", to be presented at Fifth International Geostatistics Congress, 22-27. september, 1996, Wollongong, Australia.

Omre, H., Tjelmeland, H., Qi, Y. and Hinderaker, L. (1993) "Assessment of uncertainty in the production characteristics of a sandstone reservoir", in Linville, B., Burchfield, T.E. and Wesson, T.C. (eds.) *Reservoir Characterization III, Proceedings Third International Reservoir Characterization Technical Conference*, PennWellBooks, Tulsa, USA, 556-603.

Ripley, B.D. (1987). *Stochastic Simulation*, Wiley, New York, 237p.

Ripley, B.D. (1992). "Stochastic models for the distribution of rock types in petroleum reservoirs", in Walden, A.T. and Guttorp, P. (eds) *Statistics in the environmental & earth sciences*, Edvard Arnold, London.

Syversveen, A.R. and Omre, H. (1994). "Marked point models with complex conditioning used for modelling of shales", presented at 4th European Conference on the Mathematics of Oil Recovery, Røros, Norway, 7-10. june 1994.

Tjelmeland, H. (1996). "Stochastic models in reservoir characterization and Markov random fields for compact objects", Dr.ing. thesis, 1996:44, Norwegian University of Science and Technology, Trondheim, Norway, 84p.

Tjelmeland, H. and Besag, J. (1996). "Markov random fields with higher order interactions", Technical report, Statistics No. 1/1996, Norwegian University of Science and Technology, Trondheim, Norway.

Tjelmeland, H. and Holden, L. (1993). "Semi-Markov random fields", in Soares, A. (ed.) *Geostatistics Tróia '92*, Kluwer Academic Publishers, 479-491.

Younes, L. (1991). "Parameter estimation for imperfectly observed Gibbs fields and some comments on Chalmond's EM Gibbsian algorithm", in Barone, P., Frigessi, A. and Piccioni, M. (eds.) *Stochastic models, statistical methods, and algorithms in image analysis*, Lecture Notes in Statistics, **74**, Springer Verlag, 240-258.